Nishimori's Cat: Stable Long-Range Entanglement from Finite-Depth Unitaries and Weak Measurements

Guo-Yi Zhu, Nathanan Tantivasadakarn, Ashvin Vishwanath, Simon Trebst, and Ruben Verresen

Nishimori's cat: stable long-range entanglement from finite-depth unitaries and weak measurements

Guo-Yi Zhu,[1, *] Nathanan Tantivasadakarn,[2, 3] Ashvin Vishwanath,[3] Simon Trebst,[1, 4] and Ruben Verresen[3]

[1]*Institute for Theoretical Physics, University of Cologne, Zülpicher Straße 77, 50937 Cologne, Germany*
[2]*Walter Burke Institute for Theoretical Physics and Department of Physics,*
California Institute of Technology, Pasadena, CA 91125, USA
[3]*Department of Physics, Harvard University, Cambridge, MA 02138, USA*
[4]*Center for Computational Quantum Physics, Flatiron Institute, 162 5th Avenue, New York, NY 10010, USA*
(Dated: October 16, 2023)

In the field of monitored quantum circuits, it has remained an open question whether finite-time protocols for preparing long-range entangled (LRE) states lead to phases of matter which are stable to gate imperfections, which can convert projective into weak measurements. Here we show that in certain cases, long-range entanglement persists in the presence of weak measurements, and gives rise to novel forms of quantum criticality. We demonstrate this explicitly for preparing the two-dimensional (2D) GHZ cat state and the three-dimensional (3D) toric code as minimal instances. In contrast to random monitored circuits, our circuit of gates and measurements is deterministic; the only randomness is in the measurement outcomes. We show how the randomness in these weak measurements allows us to track the solvable Nishimori line of the random-bond Ising model, rigorously establishing the stability of the glassy LRE states in two and three spatial dimensions. Away from this exactly solvable construction, we use hybrid tensor network and Monte Carlo simulations to obtain a non-zero Edwards-Anderson order parameter as an indicator of long-range entanglement in the 2D scenario. We argue that our protocol admits a natural implementation in existing quantum computing architectures, requiring only a depth-3 circuit on IBM's heavy-hexagon transmon chips.

In extended quantum systems, the rich interplay between measurements and quantum correlations point to a plethora of new emergent phenomena. Although measurements are often associated with reducing entanglement, they provide an intriguing loophole enabling fast preparation of long-range entangled (LRE) states – such as macroscopic cat states or topologically ordered states – that are otherwise forbidden. Indeed, while LRE can only be prepared with a unitary quantum circuit whose *depth grows with system size*[1–10], a large class of them can be prepared in *finite time* by simply measuring certain *stabilizers*[11][12]. This allows for deterministic state preparation using a finite-depth unitary feedback[13–19], intimately tied to the idea of quantum error correcting codes[20, 21]. Moreover, it has recently been shown that measurement-based state preparation protocols also exist for certain non-stabilizer states, including non-Abelian topological order[22–25].

Remarkably, it is not known whether such measurement-induced states form stable phases of matter, which are robust to local perturbations of the preparation protocol. While this question is of clear practical significance, it is also of conceptual interest to explore whether one can extend the familiar notion of stability of phases of matter (primarily developed for solid-state purposes) to the era of quantum simulators and computers[26, 27]. Here, we explore what happens when the circuit is perturbed prior to measuring. In effect, this turns an originally projective measurement into a weak measurement, as we will discuss. We ask whether such a generic scenario allows for stable LRE states; and if so, is there a critical point at the boundary of stability?

This motivating question fits naturally into the broader realm of monitored quantum circuits[28, 29]. Recent years have seen immense progress and activity in studying the long-time limit of random unitary gates combined with (projective) measurements. A key result has been that there is an entanglement transition between volume-law and area-law entangled regions as one increases the measurement rate[30, 31]. Subsequent works also explored how the latter can be in distinct phases of matter[32–37]. While the effects of weak measurements have been partially explored for the case of long-time quantum trajectories[38–47], to the best of our knowledge, it has not been explored in the *finite-time* protocols. This question is especially important in the latter case, since using measurement is then the *only* route towards preparing LRE states.

In this Letter, we establish a stability threshold for various measurement based protocols that induce long range entanglement, with a novel form of quantum criticality at the threshold. For this it is of fundamental importance to recall how one experimentally measures a multi-body stabilizer $\mathcal{O}$ for an arbitrary state $|\psi\rangle$, such as the two-body Ising interaction for a cat state[13] or the four-body stabilizers of the toric code[49]. Since most platforms naturally perform *single-site measurements*, one introduces an ancilla qubit and entangles it with $|\psi\rangle$ in such a way that measuring the ancilla effectively measures $\mathcal{O}$. However, if the entangling operation is not perfect, the net result is to have a (partial collapsing) *weak measurement*[50]. This can be seen most clearly from the following identity that transforms real time into imaginary time evolution up to a complex phase factor (derived in the Supplemental Material (SM)[51])

$$\langle \pm_y | e^{-it s^z \otimes \mathcal{O}} | +_x \rangle \propto e^{\pm \frac{\beta}{2} \mathcal{O}} \text{ with } \tanh(\beta/2) = \tan t, \quad (1)$$

where $|\pm_\alpha\rangle$ are the eigenstates of Pauli matrix s^α on the ancilla qubit. This is a projective measurement on $|\psi\rangle$ *only* if
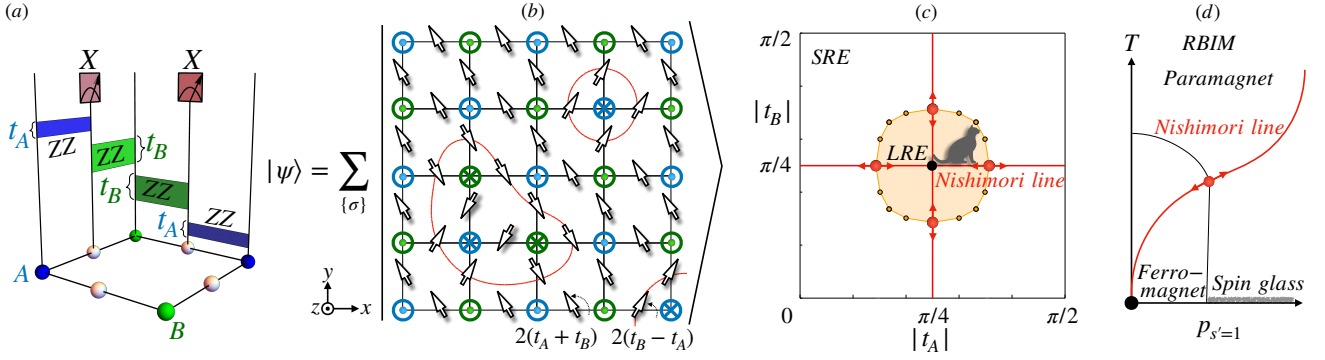
FIG. 1. **Circuit and phase diagram for Nishimori's cat from measurements**. (a) On the Lieb lattice populated with physical site (blue/green) and ancilla bond (white) spins, a depth-4 circuit of e^{-itZZ} gates is applied to nearest-neighbor spins, where the evolution time depends on the site sublattice (A/B), and the ancilla bond spins are then measured in Pauli-x basis. (b) A classical snapshot of the pre-measurement wavefunction. The circles/crosses label spins up($\uparrow$)/down($\downarrow$), and their domain walls are highlighted by red loops. Ising evolution correlates the ancillae to the domain walls. (c) Wavefunction phase diagram and the Nishimori line by tuning evolution times on the A(B) sublattice. The post-measurement wavefunction is a LRE disordered cat state inside the yellow region, and a short-ranged entangled (SRE) state outside. A Z_2 gauge symmetry emerges along the Nishimori lines (red), which upon gauge symmetrization, can be mapped exactly onto the eponymous line[48] in the phase diagram of the classical RBIM shown in (d). Beyond the Nishimori line, the phase boundaries in (c) are charted out by numerical computations (yellow dots), which have no direct equivalent in the RBIM phase diagram.

$t = \frac{\pi}{4}$: then $\beta = \infty$ pins $\mathcal{O} = \pm 1$ depending on the measurement outcome. Eq. (1) gives us two key insights into the correlations resulting from weak measurements (e.g., for times $0 < t < \pi/4$): first, the effective imaginary time-evolution suggests we ought to consider phases which are stable to finite temperature, such as a 2D Ising ferromagnet or 3D discrete gauge theory. Second, the randomness of measurement outcomes introduces effective disorder. A large part of our analysis is devoted to demonstrating stability against this disorder, which we discuss in detail for the minimal cases of a 2D GHZ-type[52] state, and whose discussion *mutatis mutandis* carries over for the 3D toric code. Crucially, the disorder distribution in our scenario is highly correlated, enabling us to map the entire range between strong and weak measurements $\pi/4 \geq t \geq 0$ *exactly* onto the solvable Nishimori line of the random bond Ising model (RBIM)[48]. For instance, for the simple protocol in Eq. (1), we find a Nishimori critical point at $t_c \approx 0.143\pi$ in 2D. We refer to the stable LRE phase between the GHZ-type fixed point and the Nishimori critical point as *Nishimori's cat*. Our work thereby also establishes a firm connection between monitored circuits and the vast literature on spin glasses.

Prior work.– We further note that finite-time transitions have recently been explored in the context of teleportation transitions[53, 54], which again involves projective measurements and where one leaves a *subextensive* region unmeasured, while Ref. 55 studied the effect of weak measurement on *removing* quantum correlations of an initially critical state. Finite-depth transitions have also been explored in the context of computational[56] and complexity transitions[57]. Finally, we point out an intriguing formal connection to phase transitions in information recovery in surface codes[21], where in the absence/presence of syndrome measurement errors, the problem is also mapped to the 2D RBIM/3D random plaquette Ising gauge model along the Nishimori line.

Circuit model.– To achieve an Ising LRE phase, we weakly measure the domain wall operator: $\mathcal{O} = \sigma_i^z \sigma_j^z$, which is weight-three when including additional ancillae (see Eq. (1)). However, one can design a protocol with only two-body evolutions[51]. For this, we consider qubits on the Lieb lattice (Figure 1a), where we denote the target spins on the square lattice as $\sigma_j^{z(x)}$ and the ancillae at the bond centers as $s_{ij}^{z(x)}$. We entangle these two types of spins by a depth-4 circuit of nearest-neighbor Ising evolutions (Fig. 1a):

$$|\psi(t_A, t_B)\rangle = e^{-i\sum_{\langle ij\rangle} t_j \sigma_j^z s_{ij}^z} |+_x\rangle^{\otimes N} . \quad (2)$$

Crucially, we have introduced *two* evolution times $t_j = t_{A(B)}$ if j belongs to the A or B sublattice (of the original square lattice of site spins), see Fig. 1a. As shown in Fig. 1b, the pair of gates associated with any given bond effectively rotates the ancilla spin by an angle $2(t_A \pm t_B)$ depending on the alignment of the neighboring spin pair. Consequently, measuring the ancilla spin in x direction weakly measures the domain wall of the target spins, which becomes a strong measurement only when both $t_A, t_B \to \frac{\pi}{4}$, in which case $|\psi\rangle$ equals the 2D cluster state[13]. More generally, the entire wavefunction (2) can be viewed as a superposition of all allowed $\{\sigma\}$ classical configurations, in which the orientation of ancillae uniquely depends on whether it sits on a domain wall or not (Fig. 1b).

The probability of the measurement outcome $s_{ij}^x \to s_{ij} = \pm 1$ is given by Born's rule:

$$p_{\{s\}} \equiv \|\langle\{s\}|\psi\rangle\|^2 \propto \sum_{\{\sigma\}} e^{-\beta\sum_{ij}(J_{s_{ij}}\sigma_i\sigma_j + hs_{ij})} , \quad (3)$$

which we recognize as the partition function of the RBIM (with the measurement outcome labeling the random bond configuration), where a straightforward computation[51]

shows that

$$\tanh \frac{\beta}{2} J_+ = \tan t_A \tan t_B, \quad \tanh \frac{\beta}{2} J_- = -\tan t_A \cot t_B,$$

and $\beta h = \frac{1}{2} \ln|\tan(t_A + t_B)\tan(t_A - t_B)|$. The subspace $(t_A, t_B = \pi/4)$ of this two-parameter protocol recovers the single-parameter protocol of Eq. (1). Note that we can interpret the right-hand side of Eq. (3) as a classical partition function $Z_{\{s\}}$, which contains the information of all diagonal correlation functions[58–60] of our post-measurement quantum state.

We can thus interpret the ensemble (over all measurement outcomes of the ancillae) as a classical system with disorder $\{s\}$, where frustrated plaquettes $\prod_{l \in \square} s_l = -1$ are said to have an Ising vortex. However, unlike commonly studied disordered models, the disorder distribution in Eq. (3) is highly correlated (making the vortices attractive). In fact, the property that $Z_{\{s\}} \propto p_{\{s\}}$ is akin to the structure Nishimori first uncovered after a gauge transformation [48] for his eponymous line in the RBIM. It implies that certain quantities (like the internal energy) are non-singular even at the transition. This remarkable fact is naturally explained by our approach, since those quantities can be expressed as *linear* functions of the density matrix of the pre-measurement wavefunction, generated by finite-depth unitary circuit.

To chart out our generic phase diagram in Fig. 1c, we use the Edwards-Anderson (EA) order parameter as our diagnostic for the formation of a glassy LRE state[61]:

$$q \equiv [\langle \sigma_0 \sigma_c \rangle^2] \equiv \sum_{\{s\}} p_{\{s\}} \langle \sigma_0 \sigma_c \rangle_{\{s\}}^2, \quad (4)$$

where $\sigma_{c(0)}$ is the spin at the central(corner) site of the open square lattice, $[\cdots]$ denotes the measurement (disorder) average, and $\langle \cdots \rangle$ the quantum average of the post-measurement wavefunction, equivalent to the classical ensemble average for a given disorder pattern. Due to the global Ising symmetry of the protocol, the quantum state is Ising symmetric with $\langle \sigma \rangle = 0$, and a nonzero EA order in thermodynamic limit signifies long-range connected quantum correlation, which serves as lower bound for the quantum mutual information between two sites at a distance[62]. Therefore the ordered phase of this classical description corresponds to the post-measurement quantum state being a LRE cat state.

Nishimori line.– Along the line $(t_B = \pi/4)$ (the red horizontal line in Fig. 1c, although the same discussion also applies to $t_A = \pi/4$), the EA order parameter can be exactly mapped to the magnetization of the Nishimori line in the RBIM, which exhibits a phase transition on crossing the Nishimori multicritical point[63–71]. Importantly, this point is located at a finite $t_A < \pi/4$ in our model, implying stability of the cat state up to a *finite* error threshold at $t_A^c \approx 0.143\pi$[48, 66–72]. This can be seen as follows: Firstly, consider the partition function (3) for a given disorder realization. Then as $\beta J_+ = -\beta J_-$ and $\beta h = 0$, our circuit model becomes precisely equivalent to the RBIM with quenched binary bond disorder, where the inverse temperature $\beta \equiv \ln|\tan(t_A + \pi/4)|$ (by setting $J_+ = -J_- = 1$) is tuned by the unitary evolution time. Secondly, consider the disorder ensemble: due to an Ising gauge symmetry in the pre-measurement wavefunction[51], any pair of bond disorder configurations that share the same vortex configuration are gauge equivalent and have the same probability. Together, this implies that our possible measurement outcomes $\{s\}$ form a gauge symmetric disorder ensemble generated by *gauge symmetrizing* an *uncorrelated* bond disorder $\{s'\}$ with probability $p_{s'=1} = 1/(1 + e^{2\beta}) = (1 - \sin(2t_A))/2$, according to

$$\sigma'_j = \sigma_j \tau_j, \quad s'_{ij} = s_{ij}\tau_i\tau_j, \quad (5)$$

where $\tau_j = \pm 1$ stands for a local Z_2 gauge transformation. Then the measurement average can be decomposed to two steps: $[\cdots] = \sum_{\{\tau\}} [\cdots]'$, where $[\cdots]'$ denotes the uncorrelated disorder average as in the RBIM, and $\sum_{\{\tau\}}$ denotes gauge symmetrization. We thus find that all gauge invariant observables of the Nishimori line in the RBIM (i.e. the red line in Fig. 1d) coincide with those in our model.

The Nishimori line is known to be invariant under a renormalization group flow[72, 73], which crosses the paramagnetic/ferromagnetic phase boundary at a multicritical point[48, 67, 74]. It was mathematically proven that the phase transition happens at *finite* critical disorder probability[21, 48, 75]. Inside the ferromagnetic phase, $[\langle \sigma_0 \sigma_c \rangle]' \neq 0$. Nevertheless, our wavefunction measurement average involves an extra gauge symmetrization, i.e. summation over $\tau = \pm 1$, which turns the ferromagnetic phase into a finite-temperature spin glass: $[\langle \sigma_0 \sigma_c \rangle] = 0$, $[\langle \sigma_0 \sigma_c \rangle^2] \neq 0$. That is, while the linear magnetization vanishes, the *non-linear* EA order parameter keeps track of the magnetization correlation in each gauge sample, because $[\langle \sigma_0 \sigma_c \rangle^2] = [\langle \sigma_0 \sigma_c \rangle^2]' = [\langle \sigma_0 \sigma_c \rangle]'$[48]. More generally, any odd moment of a σ correlation function is odd under gauge transform and thus vanishes under gauge symmetrization. Note that this spin glass state should be contrasted to the zero-temperature spin glass in the 2D RBIM (indicated by the gray dashed line in Fig. 1e). The robust glassiness of our state against finite temperature originates from the gauge symmetry, analogous to the exactly solvable Mattis spin glass[65, 76] which gauge symmetrizes the frustration-free Ising ordered phase. Nevertheless, away from the limit $t_A \to \pi/4$, our state features a finite density of Ising vortices which is more nontrivial than conventional Mattis spin glasses.

Beyond the Nishimori line.– We expect the phase diagram established on the Nishimori line to be perturbatively robust, because any symmetric perturbation in the circuit away from the Nishimori line can be mapped to a local, Ising-symmetric perturbation in the corresponding classical model. For more generic (t_A, t_B), the partition function $Z_{\{s\}}$ of Eq. (3) can still be interpreted as a disordered Ising model, albeit one with imbalanced strengths, J_+ and J_-, of the ferro- and antiferromagnetic bonds signaling the breakdown of the gauge symmetry, i.e. we are moving away from the solvable line in the phase diagram of Fig. 1c (and out of the plane of the phase
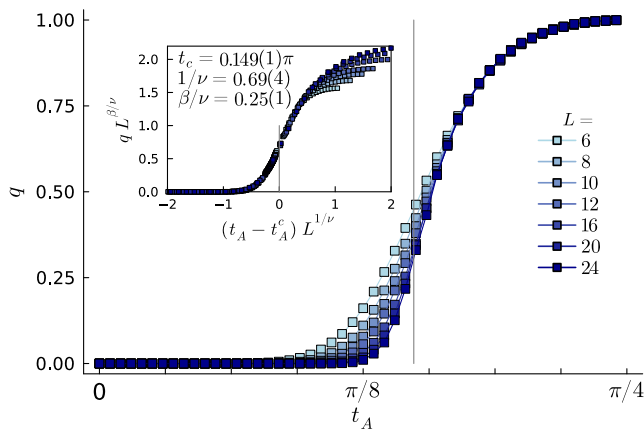
FIG. 2. **Transition from SRE to LRE states after finite evolution time along the Nishimori line** $(t_A, t_B = \pi/4)$ in the phase diagram of Fig. 1(d). Shown are results for the EA order parameter from our hybrid Monte-Carlo / tensor-network approach (symbols) for Lieb lattices of varying system sizes with open boundaries. The vertical grey line indicates our estimate of the critical point $t_c \approx 0.149\pi$ extracted from a data collapse in a window $0.1\pi \le t_A \le 0.2\pi$, fitting a scaling function[77] $q = \left[\langle \sigma_0 \sigma_c \rangle^2\right] \propto L^{-\beta/\nu} f((t_A - t_A^c)L^{1/\nu})$.

diagram in Fig. 1d). Indeed, while the 'Nishimori property' $p_{\{s\}} \propto Z_{\{s\}}$ remains, the gauge symmetry was crucial for obtaining exact results along the Nishimori line[48]. This coupling imbalance becomes particularly pronounced when one approaches the diagonal line $t_A = t_B$ in the phase diagram of Fig. 1c, where the strength of the ferromagnetic bond diverges to infinity.

For this generic scenario with two time scales (t_A, t_B), one needs to numerically contract out the *entire* tensor network to calculate the disorder probability $p_{\{s\}}$, which is essentially a structured shallow version of the quantum circuit sampling problem [78–80]. To do so, we develop a hybrid Monte-Carlo/tensor-network approach, which traces out the two degrees of freedoms in different manners: We sample the ancilla bond spins $\{s\}$ using a standard Metropolis algorithm but the weights of the importance sampling are computed by tracing out the site spins $\{\sigma\}$ via a tensor-network algorithm (for details of the algorithm see SM[51]). Despite the considerable cost of such Monte Carlo sweeps, this treatment has the advantage that it effectively avoids the minima of the glassy landscape for the $\{\sigma\}$ spins in the presence of disorder [81].

We use this method to chart out the phase diagram in Fig. 1c by performing calculations for three scenarios: along the Nishimori line $t_B = \pi/4$ (to validate our approach), along the diagonal line $t_B = t_A$ (with maximal coupling imbalance), as well as for a case in-between with $t_B = \pi/5$. Along the Nishimori line, varying the system size and analyzing the finite-size scaling of the EA order parameter as shown in Fig. 2, we can verify the existence of a true *critical point* at $t_A^c \approx 0.149\pi$, in reasonable numerical agreement with the location of the multicritial Nishimori point established in large-scale simulations[48, 66–72] of the RBIM identifying the crit-

ical point $t_A^c \approx 0.143\pi$ and $\nu \approx 4/3$. The numerical results for the diagonal line $t_B = t_A$ and $t_B = \pi/5$ are qualitatively similar and provided in SM[51].

Realization in quantum devices.– Vying a potential realization of our 2D cat state construction, we note that our protocol employs two basic ingredients that are readily available in current digital quantum computing platforms: a two-body Ising evolution and selective measurements for an extensive set of ancilla qubits on every bond. A particularly well-suited platform is IBM's quantum computing systems[27], which arrange their superconducting transmon qubits in a heavy-hexagon lattice geometry – a honeycomb variant of the square Lieb lattice, which can be realized by a depth-3 circuit and exhibits qualitatively similar physics as discussed above, exhibiting a smaller LRE phase region (for detailed calculations see the SM[51]). An important question is how to experimentally prove the successful preparation of a LRE state. Along the Nishimori line, a large number of distinct ancillae configurations are related by the gauge transformation such that the classical spin snapshot for one ancilla configuration can be transformed to that for another gauge equivalent configuration. The current chip sizes (with up to 127 qubits), allow a brute-force approach by post-selecting[82] the same ancillae vortex configuration to measure the EA order, which at worst case costs $O(2^Q)$ number of operations with $Q = 18$ being the number of plaquettes. Note the probability of obtaining vortex-free configuration approaches 100% when $t_A \to \pi/4$.

Glassy topological order.– As the 2D Ising protocol measuring domain walls generates Nishimori's cat state with Ising vortex disorder, an analogous 3D gauge protocol that weakly measures plaquette fluxes[83] results in a glassy Z_2 topological order[84, 85] with magnetic monopole disorder[21]. For instance, using Eq. (1) for the four-body plaquette stabilizer $\mathcal{O} = B_p$ of the toric code on the cubic lattice, results in the correlations of classical 3D Z_2 lattice gauge theory (describing the fluctuation of magnetic flux tubes). The latter is well-known to have a finite-temperature transition[86, 87] in the clean case. Our correlated disorder distribution is by construction (and like the 2D case) of Nishimori type, which allows us to directly relate the post-measurement state to the solvable line of the classical 3D random plaquette Z_2 gauge model[51]. This has an extended deconfined phase with a known transition[21, 75, 88] which, mapped to our time parametrization, occurs at $t_c \approx 0.192\pi$. For times beyond this critical threshold, we have stable topological order, which can be detected by the perimeter law scaling of the EA analogue of the Wilson loop. We note that this protocol only (weakly) measures fluxes; gauge charges remain frozen and absent at all times. See the SM for more details, in particular, how the above solvable path can be achieved using only three-body gates[51].

Outlook.– We have demonstrated that stable LRE phases (2D cat states and 3D topological order) can be realized in fixed-depth unitaries upon relaxing strong to weak measurements. The key conceptual finding is that weak measurements can effectively act as a source of thermal fluctuations and cor-

related disorder that conspire to yield precisely Nishimori's critical state. The stability of the ordered phase in the classical model implies that the cat state is stable against generic Ising symmetric noise, a detailed study of which is left to future study. Unlike deep-depth random unitary circuits which feature fluctuations in the temporal dimension, our state exhibits criticality with fluctuations solely in space, reminiscent of projected-entangled-paired-state *wavefunction deformation criticality*[58–60, 89–94] effectively tuned by a deterministic circuit.

Although the focus of the present work was on stable measurement-induced LRE, we note that our mechanism can be used more generally to prepare exotic states, such as *deterministically* preparing phase transitions between distinct stable SRE phases in 1D[95–97], or symmetry-enriched cat states in higher dimensions[98], see SM for details[51]. More generally, it would be interesting to further explore how weak measurements can give rise to new phenomenology in monitored circuits.

We emphasize the implementability of our protocol, with regard to the heavy-hexagon geometry of the IBM transmon chips, which will require only a depth-3 circuit to bring Nishimori's cat to life. Alternatively, Rydberg atom simulators are a highly tunable platform[99–101] allowing for measuring ancillae[102–104]. The Ising interactions of Rydbergs on sites and bonds of a hexagonal lattice have been argued to generate the requisite unitary evolution[22], making this a promising platform for realizing this transition. While the EA order parameter can in principle be measured in a brute-force manner for current chip sizes, an important open question is whether post-selection can be effectively avoided, e.g., by engineering a clever decoder for reading out hidden information[105–109]. To implement a minimal instance of glassy topological order via a 3D 'Nishimori code', we anticipate that a two-body Ising evolution on the Raussendorf lattice[110] is sufficient to give a stable toric code phase in 3D.

Note added.– Upon completion of the present manuscript, we became aware of an independent work studying extended long-range entangled phases and transitions from finite-depth unitaries and measurement, which will appear in the same arXiv posting [111].

---

* gzhu@uni-koeln.de

[1] S. Bravyi, M. B. Hastings, and F. Verstraete, Lieb-Robinson Bounds and the Generation of Correlations and Topological Quantum Order, Phys. Rev. Lett. **97**, 050401 (2006).

[2] M. Aguado and G. Vidal, Entanglement Renormalization and Topological Order, Phys. Rev. Lett. **100**, 070404 (2008).

[3] R. König, B. W. Reichardt, and G. Vidal, Exact entanglement renormalization for string-net models, Phys. Rev. B **79**, 195123 (2009).

[4] X. Chen, Z.-C. Gu, and X.-G. Wen, Local unitary transformation, long-range quantum entanglement, wave function renormalization, and topological order, Phys. Rev. B **82**, 155138 (2010).

[5] M. P. Zaletel and F. Pollmann, Isometric Tensor Network States in Two Dimensions, Phys. Rev. Lett. **124**, 037201 (2020).

[6] T. Soejima, K. Siva, N. Bultinck, S. Chatterjee, F. Pollmann, and M. P. Zaletel, Isometric tensor network representation of string-net liquids, Phys. Rev. B **101**, 085117 (2020).

[7] Y.-J. Liu, K. Shtengel, A. Smith, and F. Pollmann, Methods for simulating string-net states and anyons on a digital quantum computer, (2021), arXiv:2110.02020.

[8] Z.-Y. Wei, D. Malz, and J. I. Cirac, Sequential Generation of Projected Entangled-Pair States, Phys. Rev. Lett. **128**, 010607 (2022).

[9] K. X. Wei, I. Lauer, S. Srinivasan, N. Sundaresan, D. T. McClure, D. Toyli, D. C. McKay, J. M. Gambetta, and S. Sheldon, Verifying multipartite entangled greenberger-horne-zeilinger states via multiple quantum coherences, Phys. Rev. A **101**, 032343 (2020).

[10] G. J. Mooney, G. A. L. White, C. D. Hill, and L. C. L. Hollenberg, Generation and verification of 27-qubit greenberger-horne-zeilinger states in a superconducting quantum computer, Journal of Physics Communications **5**, 095004 (2021).

[11] Which are finite products of Pauli operators.

[12] D. Gottesman, Stabilizer Codes and Quantum Error Correction (1997), arXiv.quant-phys:9705052.

[13] H. J. Briegel and R. Raussendorf, Persistent Entanglement in Arrays of Interacting Particles, Phys. Rev. Lett. **86**, 910 (2001).

[14] R. Raussendorf, S. Bravyi, and J. Harrington, Long-range quantum entanglement in noisy cluster states, Phys. Rev. A **71**, 062313 (2005).

[15] M. Aguado, G. K. Brennen, F. Verstraete, and J. I. Cirac, Creation, Manipulation, and Detection of Abelian and Non-Abelian Anyons in Optical Lattices, Phys. Rev. Lett. **101**, 260501 (2008).

[16] G. K. Brennen, M. Aguado, and J. I. Cirac, Simulations of quantum double models, New Journal of Physics **11**, 053009 (2009).

[17] A. Bolt, G. Duclos-Cianci, D. Poulin, and T. M. Stace, Foli-

ated Quantum Error-Correcting Codes, Phys. Rev. Lett. **117**, 070501 (2016).

[18] L. Piroli, G. Styliaris, and J. I. Cirac, Quantum Circuits Assisted by Local Operations and Classical Communication: Transformations and Phases of Matter, Phys. Rev. Lett. **127**, 220503 (2021).

[19] A. J. Friedman, C. Yin, Y. Hong, and A. Lucas, Locality and error correction in quantum dynamics with measurement, arXiv:2206.09929.

[20] D. Gottesman, A. Kitaev, and J. Preskill, Encoding a qubit in an oscillator, Phys. Rev. A **64**, 012310 (2001).

[21] E. Dennis, A. Kitaev, A. Landahl, and J. Preskill, Topological quantum memory, Journal of Mathematical Physics **43**, 4452 (2002).

[22] R. Verresen, N. Tantivasadakarn, and A. Vishwanath, Efficiently preparing Schrödinger's cat, fractons and non-Abelian topological order in quantum devices, (2021), arXiv:2112.03061.

[23] N. Tantivasadakarn, R. Thorngren, A. Vishwanath, and R. Verresen, Long-range entanglement from measuring symmetry-protected topological phases, (2021), arXiv:2112.01519.

[24] S. Bravyi, I. Kim, A. Kliesch, and R. Koenig, Adaptive constant-depth circuits for manipulating non-abelian anyons, (2022), arXiv:2205.01933.

[25] T.-C. Lu, L. A. Lessa, I. H. Kim, and T. H. Hsieh, Measurement as a shortcut to long-range entangled quantum matter, (2022), arXiv:2206.13527.

[26] E. Altman, K. R. Brown, G. Carleo, L. D. Carr, E. Demler, C. Chin, B. DeMarco, S. E. Economou, M. A. Eriksson, K.-M. C. Fu, M. Greiner, K. R. Hazzard, R. G. Hulet, A. J. Kollár, B. L. Lev, M. D. Lukin, R. Ma, X. Mi, S. Misra, C. Monroe, K. Murch, Z. Nazario, K.-K. Ni, A. C. Potter, P. Roushan, M. Saffman, M. Schleier-Smith, I. Siddiqi, R. Simmonds, M. Singh, I. Spielman, K. Temme, D. S. Weiss, J. Vučković, V. Vuletić, J. Ye, and M. Zwierlein, Quantum simulators: Architectures and opportunities, PRX Quantum **2**, 017003 (2021).

[27] A. D. Córcoles, A. Kandala, A. Javadi-Abhari, D. T. McClure, A. W. Cross, K. Temme, P. D. Nation, M. Steffen, and J. M. Gambetta, Challenges and Opportunities of Near-Term Quantum Computing Systems, Proceedings of the IEEE **108**, 1338 (2020).

[28] A. C. Potter and R. Vasseur, Entanglement dynamics in hybrid quantum circuits (2021).

[29] M. P. A. Fisher, V. Khemani, A. Nahum, and S. Vijay, Random Quantum Circuits, (2022), arXiv:2207.14280.

[30] Y. Li, X. Chen, and M. P. A. Fisher, Quantum Zeno effect and the many-body entanglement transition, Phys. Rev. B **98**, 205136 (2018).

[31] B. Skinner, J. Ruhman, and A. Nahum, Measurement-Induced Phase Transitions in the Dynamics of Entanglement, Phys. Rev. X **9**, 031009 (2019).

[32] A. Lavasani, Y. Alavirad, and M. Barkeshli, Measurement-induced topological entanglement transitions in symmetric random quantum circuits, Nature Physics **17**, 342 (2021).

[33] A. Lavasani, Y. Alavirad, and M. Barkeshli, Topological order and criticality in $(2+1)$D monitored random quantum circuits, Phys. Rev. Lett. **127**, 235701 (2021).

[34] S. Sang and T. H. Hsieh, Measurement-protected quantum phases, Phys. Rev. Research **3**, 023200 (2021).

[35] K. Klocke and M. Buchhold, Topological order and entanglement dynamics in the measurement-only XZZX quantum code, (2022), arXiv:2204.08489.

[36] A. Lavasani, Z.-X. Luo, and S. Vijay, Monitored Quan-

tum Dynamics and the Kitaev Spin Liquid, (2022), arXiv:2207.02877.

[37] A. Sriram, T. Rakovszky, V. Khemani, and M. Ippoliti, Topology, criticality, and dynamically generated qubits in a stochastic measurement-only Kitaev model, (2022), arXiv:2207.07096.

[38] M. Szyniszewski, A. Romito, and H. Schomerus, Entanglement transition from variable-strength weak measurements, Phys. Rev. B **100**, 064204 (2019).

[39] C.-M. Jian, Y.-Z. You, R. Vasseur, and A. W. W. Ludwig, Measurement-induced criticality in random quantum circuits, Phys. Rev. B **101**, 104302 (2020).

[40] Y. Bao, S. Choi, and E. Altman, Theory of the phase transition in random unitary circuits with measurements, Phys. Rev. B **101**, 104301 (2020).

[41] M. Szyniszewski, A. Romito, and H. Schomerus, Universality of Entanglement Transitions from Stroboscopic to Continuous Measurements, Phys. Rev. Lett. **125**, 210602 (2020).

[42] Y. Fuji and Y. Ashida, Measurement-induced quantum criticality under continuous monitoring, Phys. Rev. B **102**, 054302 (2020).

[43] S.-K. Jian, C. Liu, X. Chen, B. Swingle, and P. Zhang, Measurement-Induced Phase Transition in the Monitored Sachdev-Ye-Kitaev Model, Phys. Rev. Lett. **127**, 140601 (2021).

[44] X. Turkeshi, A. Biella, R. Fazio, M. Dalmonte, and M. Schiró, Measurement-induced entanglement transitions in the quantum Ising chain: From infinite to zero clicks, Phys. Rev. B **103**, 224210 (2021).

[45] A. Biella and M. Schiró, Many-Body Quantum Zeno Effect and Measurement-Induced Subradiance Transition, Quantum **5**, 528 (2021).

[46] T. Müller, S. Diehl, and M. Buchhold, Measurement-Induced Dark State Phase Transitions in Long-Ranged Fermion Systems, Phys. Rev. Lett. **128**, 010605 (2022).

[47] G. Kells, D. Meidan, and A. Romito, Topological transitions with continuously monitored free fermions, (2021), arXiv:2112.09787.

[48] H. Nishimori, Internal Energy, Specific Heat and Correlation Function of the Bond-Random Ising Model, Progress of Theoretical Physics **66**, 1169 (1981).

[49] A. Y. Kitaev, Fault-tolerant quantum computation by anyons, Annals of Physics **303**, 2 (2003).

[50] A. A. Clerk, M. H. Devoret, S. M. Girvin, F. Marquardt, and R. J. Schoelkopf, Introduction to quantum noise, measurement, and amplification, Rev. Mod. Phys. **82**, 1155 (2010).

[51] See the Supplemental Material for details of our circuit model and its relation to Nishimori physics, a tensor-network representation of the monitored quantum state, numerical data on and off the Nishimori line along with details on the hybrid tensor network / Monte Carlo algorithm, a discussion of the alternative heavy-hexagon lattice geometry, and the route to glassy topological order in a 3D Nishimori code.

[52] D. M. Greenberger, M. A. Horne, and A. Zeilinger, Going Beyond Bell's Theorem, in Bell's Theorem, Quantum Theory, and Conceptions of the Universe (Kluwer, 1989) pp. 69–72, arXiv:0712.0921.

[53] Y. Bao, M. Block, and E. Altman, Finite time teleportation phase transition in random quantum circuits, (2021), arXiv:2110.06963.

[54] H. Liu, T. Zhou, and X. Chen, Measurement induced entanglement transition in two dimensional shallow circuit, (2022), arXiv:2203.07510.

[55] S. J. Garratt, Z. Weinstein, and E. Altman, Measurements con-

spire nonlocally to restructure critical quantum states, (2022), arXiv:2207.09476.

[56] D. E. Browne, M. B. Elliott, S. T. Flammia, S. T. Merkel, A. Miyake, and A. J. Short, Phase transition of computational power in the resource states for one-way quantum computation, New Journal of Physics 10, 023010 (2008).

[57] J. C. Napp, R. L. La Placa, A. M. Dalzell, F. G. S. L. Brandão, and A. W. Harrow, Efficient Classical Simulation of Random Shallow 2D Quantum Circuits, Phys. Rev. X 12, 021021 (2022).

[58] C. L. Henley, From classical to quantum dynamics at Rokhsar–Kivelson points, Journal of Physics: Condensed Matter 16, S891 (2004).

[59] E. Ardonne, P. Fendley, and E. Fradkin, Topological order and conformal quantum critical points, Annals of Physics 310, 493 (2004).

[60] F. Verstraete, M. M. Wolf, D. Perez-Garcia, and J. I. Cirac, Criticality, the Area Law, and the Computational Power of Projected Entangled Pair States, Phys. Rev. Lett. 96, 220601 (2006).

[61] S. F. Edwards and P. W. Anderson, Theory of spin glasses, Journal of Physics F: Metal Physics 5, 965 (1975).

[62] M. M. Wolf, F. Verstraete, M. B. Hastings, and J. I. Cirac, Area laws in quantum systems: Mutual information and correlations, Phys. Rev. Lett. 100, 070502 (2008).

[63] A. Georges, D. Hansel, and P. Le Doussal, Exact properties of spin glasses. - I. 2D supersymmetry and Nishimori's result, J. Phys. France 46, 1309 (1985).

[64] A. Georges, D. Hansel, P. Le Doussal, and J.-P. Bouchaud, Exact properties of spin glasses. II. Nishimori's line : new results and physical implications, J. Phys. France 46, 1827 (1985).

[65] K. Binder and A. P. Young, Spin glasses: Experimental facts, theoretical concepts, and open questions, Rev. Mod. Phys. 58, 801 (1986).

[66] R. R. P. Singh and J. Adler, High-temperature expansion study of the Nishimori multicritical point in two and four dimensions, Phys. Rev. B 54, 364 (1996).

[67] S. Cho and M. P. A. Fisher, Criticality in the two-dimensional random-bond Ising model, Phys. Rev. B 55, 1025 (1997).

[68] N. Read and A. W. W. Ludwig, Absence of a metallic phase in random-bond Ising models in two dimensions: Applications to disordered superconductors and paired quantum Hall states, Phys. Rev. B 63, 024404 (2000).

[69] A. Honecker, M. Picco, and P. Pujol, Universality Class of the Nishimori Point in the 2D ±J Random-Bond Ising Model, Phys. Rev. Lett. 87, 047201 (2001).

[70] F. Merz and J. T. Chalker, Two-dimensional random-bond Ising model, free fermions, and the network model, Phys. Rev. B 65, 054425 (2002).

[71] C. Amoruso and A. K. Hartmann, Domain-wall energies and magnetization of the two-dimensional random-bond Ising model, Phys. Rev. B 70, 134425 (2004).

[72] P. Le Doussal and A. B. Harris, Location of the Ising Spin-Glass Multicritical Point on Nishimori's Line, Phys. Rev. Lett. 61, 625 (1988).

[73] P. Le Doussal and A. B. Harris, ε expansion for the Nishimori multicritical point of spin glasses, Phys. Rev. B 40, 9249 (1989).

[74] I. A. Gruzberg, N. Read, and A. W. W. Ludwig, Random-bond Ising model in two dimensions: The Nishimori line and supersymmetry, Phys. Rev. B 63, 104422 (2001).

[75] C. Wang, J. Harrington, and J. Preskill, Confinement-Higgs transition in a disordered gauge theory and the accuracy threshold for quantum memory, Annals of Physics 303, 31 (2003).

[76] D. Mattis, Solvable spin systems with random interactions, Physics Letters A 56, 421 (1976).

[77] O. Melchert, autoScale.py - A program for automatic finite-size scaling analyses: A user's guide, (2009), arXiv:0910.5403.

[78] A. P. Lund, M. J. Bremner, and T. C. Ralph, Quantum sampling problems, bosonsampling and quantum supremacy, npj Quantum Information 3, 1 (2017).

[79] A. W. Harrow and A. Montanaro, Quantum computational supremacy, Nature 549, 203 (2017).

[80] F. Pan, K. Chen, and P. Zhang, Solving the sampling problem of the sycamore quantum circuits, Phys. Rev. Lett. 129, 090502 (2022).

[81] In fact, this hybrid algorithm can be applied to more general two-dimensional measurement problems as long as the wavefunctions are within the PEPS manifold of area law entanglement entropy, and the numerical complexity remains classically tractable for shallow depth circuits [57].

[82] J. M. Koh, S.-N. Sun, M. Motta, and A. J. Minnich, Experimental Realization of a Measurement-Induced Entanglement Phase Transition on a Superconducting Quantum Processor, (2022), arXiv:2203.04338.

[83] Q. Yang and D. E. Liu, Effect of quantum error correction on detection-induced coherent errors, Phys. Rev. A 105, 022434 (2022).

[84] A. Hamma, P. Zanardi, and X.-G. Wen, String and membrane condensation on three-dimensional lattices, Phys. Rev. B 72, 035307 (2005).

[85] C. Castelnovo and C. Chamon, Topological order in a three-dimensional toric code at finite temperature, Phys. Rev. B 78, 155120 (2008).

[86] F. J. Wegner, Duality in Generalized Ising Models and Phase Transitions without Local Order Parameters, Journal of Mathematical Physics 12, 2259 (1971).

[87] J. B. Kogut, An introduction to lattice gauge theory and spin systems, Rev. Mod. Phys. 51, 659 (1979).

[88] T. Ohno, G. Arakawa, I. Ichinose, and T. Matsui, Phase structure of the random-plaquette Z2 gauge model: accuracy threshold for a toric quantum memory, Nuclear Physics B 697, 462 (2004).

[89] C. Castelnovo, S. Trebst, and M. Troyer, Topological Order and Quantum Criticality, in Understanding Quantum Phase Transitions (Taylor & Francis, 2010) pp. 169–192, arXiv:0912.3272.

[90] N. Schuch, D. Poilblanc, J. I. Cirac, and D. Pérez-García, Topological Order in the Projected Entangled-Pair States Formalism: Transfer Operator and Boundary Hamiltonians, Phys. Rev. Lett. 111, 090501 (2013).

[91] G.-Y. Zhu and G.-M. Zhang, Gapless Coulomb State Emerging from a Self-Dual Topological Tensor-Network State, Phys. Rev. Lett. 122, 176401 (2019).

[92] W.-T. Xu, Q. Zhang, and G.-M. Zhang, Tensor Network Approach to Phase Transitions of a Non-Abelian Topological Phase, Phys. Rev. Lett. 124, 130603 (2020).

[93] Q. Zhang, W.-T. Xu, Z.-Q. Wang, and G.-M. Zhang, Non-Hermitian effects of the intrinsic signs in topologically ordered wavefunctions, Communications Physics 3, 209 (2020).

[94] G.-Y. Zhu, J.-Y. Chen, P. Ye, and S. Trebst, Topological fracton quantum phase transitions by tuning exact tensor network states, (2022), arXiv:2203.00015.

[95] M. M. Wolf, G. Ortiz, F. Verstraete, and J. I. Cirac, Quantum Phase Transitions in Matrix Product Systems, Phys. Rev. Lett. 97, 110403 (2006).

[96] A. Smith, B. Jobst, A. G. Green, and F. Pollmann, Crossing a topological phase transition with a quantum computer, Phys. Rev. Research **4**, L022020 (2022).

[97] N. G. Jones, J. Bibo, B. Jobst, F. Pollmann, A. Smith, and R. Verresen, Skeleton of matrix-product-state-solvable models connecting topological phases of matter, Phys. Rev. Research **3**, 033265 (2021).

[98] N. Tantivasadakarn, R. Thorngren, A. Vishwanath, and R. Verresen, Pivot Hamiltonians as generators of symmetry and entanglement, (2021), arXiv:2110.07599.

[99] A. Browaeys and T. Lahaye, Many-body physics with individually controlled Rydberg atoms, Nature Physics **16**, 132 (2020).

[100] S. Ebadi, T. T. Wang, H. Levine, A. Keesling, G. Semeghini, A. Omran, D. Bluvstein, R. Samajdar, H. Pichler, W. W. Ho, S. Choi, S. Sachdev, M. Greiner, V. Vuletić, and M. D. Lukin, Quantum phases of matter on a 256-atom programmable quantum simulator, Nature **595**, 227 (2021).

[101] P. Scholl, M. Schuler, H. J. Williams, A. A. Eberharter, D. Barredo, K.-N. Schymik, V. Lienhard, L.-P. Henry, T. C. Lang, T. Lahaye, A. M. Läuchli, and A. Browaeys, Quantum simulation of 2D antiferromagnets with hundreds of Rydberg atoms, Nature **595**, 233 (2021).

[102] D. Bluvstein, H. Levine, G. Semeghini, T. T. Wang, S. Ebadi, M. Kalinowski, A. Keesling, N. Maskara, H. Pichler, M. Greiner, V. Vuletić, and M. D. Lukin, A quantum processor based on coherent transport of entangled atom arrays, Nature (London) **604**, 451 (2022).

[103] K. Singh, S. Anand, A. Pocklington, J. T. Kemp, and H. Bernien, Dual-element, two-dimensional atom array with continuous-mode operation, Phys. Rev. X **12**, 011040 (2022).

[104] J. T. Zhang, L. R. B. Picard, W. B. Cairncross, K. Wang, Y. Yu, F. Fang, and K.-K. Ni, An optical tweezer array of ground-state polar molecules, (2021), arXiv:2112.00991.

[105] S. Choi, Y. Bao, X.-L. Qi, and E. Altman, Quantum Error Correction in Scrambling Dynamics and Measurement-Induced Phase Transition, Phys. Rev. Lett. **125**, 030505 (2020).

[106] M. J. Gullans and D. A. Huse, Dynamical Purification Phase Transition Induced by Quantum Measurements, Phys. Rev. X **10**, 041020 (2020).

[107] C. Noel, P. Niroula, D. Zhu, A. Risinger, L. Egan, D. Biswas, M. Cetina, A. V. Gorshkov, M. J. Gullans, D. A. Huse, and C. Monroe, Measurement-induced quantum phases realized in a trapped-ion quantum computer, Nature Physics **18**, 760 (2022).

[108] H. Dehghani, A. Lavasani, M. Hafezi, and M. J. Gullans, Neural-Network Decoders for Measurement Induced Phase Transitions, (2022), arXiv:2204.10904.

[109] F. Barratt, U. Agarwal, A. C. Potter, S. Gopalakrishnan, and R. Vasseur, Transitions in the learnability of global charges from local measurements, (2022), arXiv:2206.12429.

[110] R. Raussendorf, J. Harrington, and K. Goyal, A fault-tolerant one-way quantum computer, Annals of Physics **321**, 2242 (2006).

[111] J. Y. Lee, W. Ji, Z. Bi, and M. P. A. Fisher, Measurement-Prepared Quantum Criticality: from Ising model to gauge theory, and beyond, (2022), arXiv:2208.11699.

[112] https://www.ibm.com/quantum-computing/.